DOI: 10.1002/chem.201100210

Mechanistic Studies of Pd-Catalyzed Regioselective Aryl C–H Bond Functionalization with Strained Alkenes: Origin of Regioselectivity

David I. Chai,[a] Praew Thansandote,[b] and Mark Lautens*[a]

Abstract: Mechanistic studies of a palladium-catalyzed regioselective aryl C–H functionalization of 2-pyrrole phenyl iodide with norbornene are presented. Kinetic and spectroscopic analyses together with crystallographic data provide evidence for intermediates in a proposed stepwise mechanism. On the basis of the mechanistic studies, the origin of the regioselectivity is due to a ligand exchange between I^- and HO^- on the norbornyl palladium complex. These mechanistic studies also implicate that either alkoxide or water is responsible for the formation of the palladacycle, but a reversible ring-opening–ring-closing process of the palladacycle with HX can retard the rate of reaction of a key intermediate. The significant aspects of the proposed mechanism are discussed in detail.

Keywords: C–H funtionalization · heterogeneous catalysis · norbornene · palladacycle · palladium

Introduction

Selective catalytic functionalization of aromatic C–H bonds by palladium is emerging as a powerful methodology for C–C bond formation and has obtained significant attention within the field of synthetic chemistry.[1] This method simplifies the preparation of substrates and minimizes waste production due to the avoidance of pre-functionalization of one or both of the coupling partners. In particular, the functionalization of a C–H bond *ortho* to an aryl halide is of fundamental importance in synthetic organic chemistry and has provided new synthetic variations using this method.[2,3] Thus, the treatment of aryl halide **1** with either an alkyl or aryl halide containing a functional group such as an amine, alcohol, alkene, alkyne, or aryl system in the presence of catalytic Pd^0 and excess norbornene provides functionalized aromatic carbo- and heterocycles **2** via *ortho*-C–H functionalization.[2] On the other hand, the *ortho*-C–H functionalization of aryl halide **1** with norbornene in the absence of coupling partners leads to the formation of annulated products **2′**.[3] However, if aryl halide **1** contains a nucleophilic functional group adjacent to the halide, a different regioselective annulation occurs to provide interesting cyclic systems **3** (Scheme 1).[4]

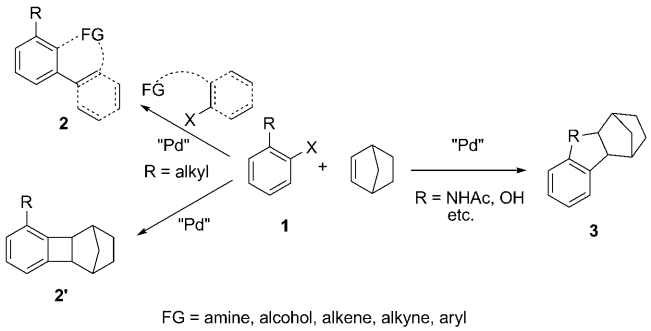

Scheme 1. Reaction of aryl halide **1** with norbornene.

In 2007, as part of an on-going project on annulation, we reported a coupling reaction between 1-(2-halophenyl)-1*H*-pyrrole (**4a**) and norbornene in the presence of $Pd(OAc)_2$ as a catalyst at 110 °C leading to annulation product **6** (Scheme 2). This reaction proceeds by the carbopalladation of aryl palladium(II) across norbornene, then a subsequent C–H functionalization of a pyrrole C–H bond (Scheme 3).[5]

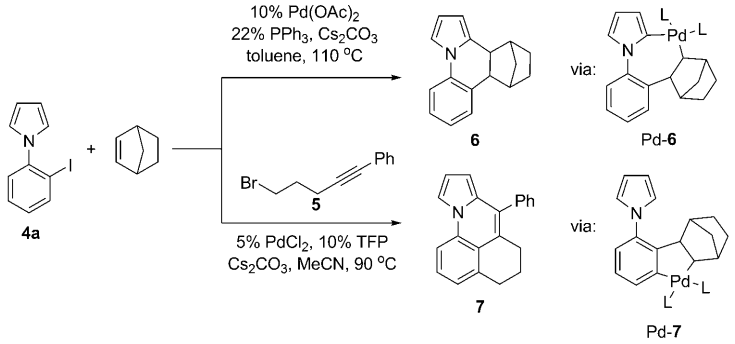

Scheme 2. Palladium-catalyzed annulation and domino reaction

[a] Dr. D. I. Chai, Prof. Dr. M. Lautens
Davenport Chemical Laboratories, Department of Chemistry
University of Toronto, 80 St. George Street
Toronto, ON M5S 3H6 (Canada)
Fax: (+1) 416-946-8185
E-mail: mlautens@chem.utoronto.ca

[b] Dr. P. Thansandote
Department of Chemistry, University of Cambridge
Lensfield Road, Cambridge, CB2 1EW (UK)

Supporting information for this article is available on the WWW under http://dx.doi.org/10.1002/chem.201100210.

Some other annulation products with other bicyclic derivatives have also been isolated. Mechanistically, we proposed that the seven-membered palladacycle Pd-**6** is formed as an intermediate in this process.

Alternatively, in a related process, we reported the synthesis of tetracyclic fused pyrroles by a palladium-catalyzed, norbornene-mediated domino reaction using pyrrole **4a** and alkyl halide **5** (Scheme 2).[21] This methodology constructed three C–C bonds in one procedure including two challenging C–H functionalizations of unactivated aryl ring systems. The proposed mechanism is based upon the formation of the five-membered palladacycle Pd-**7** according to the mechanistic studies made by Catellani and Cheng (Scheme 3).[6] As we will discuss in more detail, these two reactions share common intermediates in their early stages, but show important differences in their late stages.

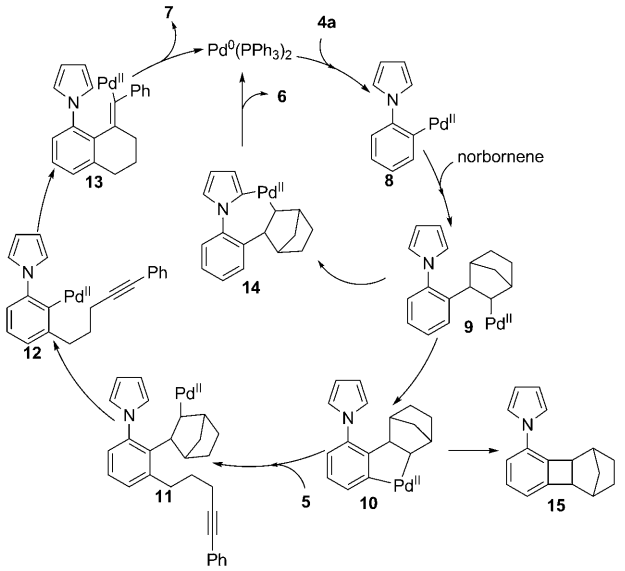

Scheme 3. Proposed mechanisms of palladium-catalyzed annulation and domino reactions. Ligands and halides are omitted for clarity.

A simplified mechanistic hypothesis for these two reactions is outlined in Scheme 3. Both catalytic cycles start with the aryl palladium complex **8**, which is formed by oxidative addition of aryl iodide **4a**. Subsequent norbornene insertion into the resulting complex **8** provides the alkyl palladium complex **9**. At this stage, the complex **9** can give rise to two regioselective intermediates **10** or **14** by a C–H functionalization. Therefore, this C–H functionalization step appears of fundamental importance for the determination of the regioselectivity. The intermediate **14** undergoes a reductive elimination to provide the annulation product **6**. The other complex **10** couples with alkyl halide **5** presumably via a Pd^{IV} intermediate to give complex **11**. Likely due to the steric effect of norbornene of complex **13**, exerted by two *ortho*-substituents, extrusion of norbornene occurs leading to complex **12**, which undergoes a cyclization to give complex **13**. The catalytic cycle is finally closed by direct arylation providing tetracyclic compound **7** and re-generating the active palladium catalyst via reductive elimination.

Due to the formation of two different C–H functionalization products from the same substrate, the conflicting regioselective palladacycle formations from complex **9** became our primary focus of interest. Thus, we began considering the controlling factors for the formation of the five-membered palladacycle **10** over the seven-membered palladacycle **14**. In view of the potential of selective *ortho* C–H functionalizations, this study would be significant to discovering new catalytic systems. To develop a simple system suitable to mechanistic studies, we decided to examine the formation of the benzocyclobutene **15**, which is formed from the palladacycle **10** by a reductive elimination (Scheme 3). Herein, we will describe detailed mechanistic studies including kinetic and NMR studies, to explain the regiomeric outcome of the reaction.

Results and Discussion

Screening and optimization study: The initial investigation of the benzocyclobutene reaction focused on using 2-pyrrole substituted phenyl bromide and norbornene while varying ligands, bases, solvents, and temperature. Whereas reactions with electron rich or neutral ligands such as $(p\text{-}MeOC_6H_4)_3P$ or PPh_3 yielded only the annulation products, the formation of the benzocyclobutene was first observed with electron-poor ligands such as $(p\text{-}CF_3C_6H_4)_3P$, but in only 1:1 selectivity of **15** and **6**. However, we discovered that the reactions with the 2-pyrrole substituted phenyl bromide and this electron poor ligand gave poor reproducibility. To our delight, the benzocyclobutene reaction was found to be both high yielding and reproducible using water as a co-solvent and hydroxide ion as a base. Interestingly, the use of the electron neutral ligand, PPh_3, led to excellent selectivity in this case. Thus, the benzocyclobutene **15** was obtained in 95% yield using 10 mol% $Pd(OAc)_2$, 22 mol% PPh_3, 4 equiv norbornene, and 2 equiv Bu_4NOH in toluene and water (1:1).

A list of the controlling factors obtained from the optimization studies for the C–H functionalization is summarized in Table 1 and interpreted in Table 2. Among the important factors governing the selectivity, the temperature and base had the most significant impact to favor the benzocyclobutene formation. It seems that the pyrrole annulation reaction can only proceed at temperatures higher than 90°C. Also, no benzocyclobutene products were observed with stronger bases such as KHMDS or KOR or weaker bases such as K_3PO_4 or K_2CO_3. It is worth noting that the formation of **15** was not observed unless the reaction was run in a sealed system.

Development of a system for mechanistic study: Upon successful optimization studies, we sought to develop a system suitable for kinetic and spectroscopic analysis of the palladium intermediates formed during the reaction. Unfortunately, the palladium intermediates **9** and **10** are not sufficiently

Table 1. Experiments to determine controlling factors for benzocyclobutene.[a]

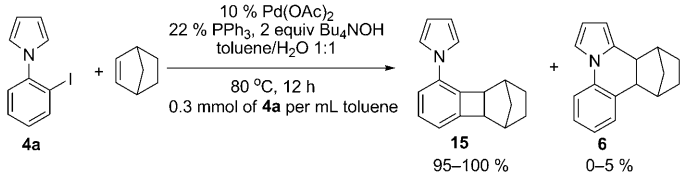

Entry	Original conditions	Changed conditions	**15** [%]	**6** [%]
1	toluene/H_2O 1:1	H_2O	100	0
2	80 °C	100 °C	0–10	90–100
3	Bu_4NOH	Cs_2CO_3	trace	30
4	Bu_4NOH	KHMDS or KOR (R = Me and *t*Bu)	0	0
5	toluene/H_2O 1:1	toluene[b]	80	20
6	aryl iodide **4a**	aryl bromide[c]	45–100[d]	0–55[d]
7	0.30 M[e]	0.15 M	50	18

[a] Measured by ^{1}H NMR. [b] KOH was used instead of Bu_4NOH. [c] 2-Pyrrole phenyl bromide was used in place of **4a**. [d] Not reproducible. [e] Concentration (mmol) of **4a** in 1 mL toluene.

Table 2. Controlling factors for aryl C–H functionalization.[a]

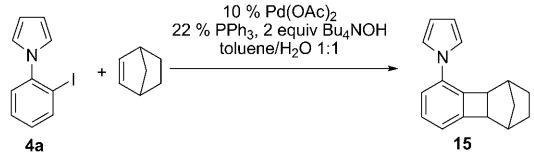

Entry	Reagent	Importance
1	solvent	choice of solvent does not control the selectivity since reactions still worked in neat conditions on water
2	temperature	important for selectivity; full conversion to **15** at 80 °C, but low selectivity at 100 °C
3	Bu_4NOH	important for selectivity; it can act as a phase-transfer reagent as well as a base. Controls the basicity of organic layer.
4	water	low selectivity without water; removes by-products such as HX (X = OAc or I)
5	halide	Aryl bromide gave un-reproducible results; aryl iodide necessary for reproducible results
6	concentration	0.3 M or higher concentration required for full conversion; negligible variations in selectivity.

[a] Reactions were conducted on 0.15 mmol scale with $Pd(OAc)_2$ (10 mol %), PPh_3 (22 mol %), Bu_4NOH (0.3 mmol), toluene (0.5 mL), H_2O (0.5 mL), and norbornene (0.6 mmol).

stable to isolate, presumably due to steric hindrance between the pyrrole and norbornyl moieties. Thus, we decided to focus on synthesizing palladium complexes with unsubstituted phenyl iodides to use for our mechanistic studies.

For high-yielding reactions with minimal byproduct formation, we modified the optimized reaction conditions in the following ways: 1) a stoichiometric $[Pd(PPh_3)_4]$ catalyst was used instead of $Pd(OAc)_2/PPh_3$ mixture to avoid the reduction of Pd^{II} to Pd^0 and the potential competitive coordination between acetate and iodide ions for the palladium complexes. 2) The mechanistic studies were conducted from the substrate immediately leading to each intermediate of interest. 3) Changes in reaction conditions were made when necessary such as switching the solvent to overcome solubility issues, lowering the temperature to avoid decomposition of the intermediates, and changing the base to increase the reaction rate. To correlate the proposed mechanism to the original reaction conditions, the crude NMR data obtained from reactions of 1-(2-iodophenyl)-1*H*-pyrrole (**4a**) under the optimized reaction conditions were used to compare with the data obtained for our model substrate. It is worth noting that attempts to take the kinetic study of the full catalytic cycle were unsuccessful due to the significant formation of by-products.

Kinetic analysis of carbopalladation steps: ***Step 1***: To determine possible intermediates and obtain mechanistic insight for the carbopalladation step, we monitored the reaction between aryl palladium complexes and norbornene at variable temperatures by ^{1}H and ^{31}P NMR spectroscopy. The relative rates of the carbopalladation of the isolated palladium complexes (Pd-**1**) were studied with 1.5 equiv of norbornene in $CDCl_3$ (Figure 1). All reactions represented here showed no or little induction period and all reaction rates were measured after the reaction was initiated.

The rates of carbopalladation conducted with Pd-**1** varying electronics and sterics are illustrated by curves in Figures 1 and 2. The kinetics of the carbopalladation was consistent with the reaction being second order. The second-order kinetic Equation (1) can be obtained by considering excess norbornene with respect to Pd-**1**, where x is the molar fraction of Pd-**1** at t (i.e., $x = [\text{Pd-}\mathbf{1}]_t/[\text{Pd-}\mathbf{1}]_0$) (see Supporting Information for derivation).

$$\ln\left(1+\frac{0.5}{x}\right) = \ln(1.5) + \frac{k_{app}[\text{Pd-}\mathbf{1}]_0}{2}t \qquad (1)$$

$$x = [\text{Pd-}\mathbf{1}]_t/[\text{Pd-}\mathbf{1}]_0$$

As shown in Figure 2, the plot of $\ln(1+(1/(2\cdot x)))$ versus time shows a linear plot with slope equal to $k_{app}\cdot[\text{Pd-}\mathbf{1}]_0/2$ for the carbopalladation step, but slightly deviates from the linear plot over time. Clearly, the relative rates of Pd-**1** with different electronic properties follow the order: Pd-**1b** ($k_{app} = 0.0798\ \text{M}^{-1}\text{min}^{-1}$) > Pd-**1a** ($k_{app} = 0.018\ \text{M}^{-1}\text{min}^{-1}$) > Pd-**1c** ($k_{app} = 0.00336\ \text{M}^{-1}\text{min}^{-1}$) at 25 °C, which suggests that

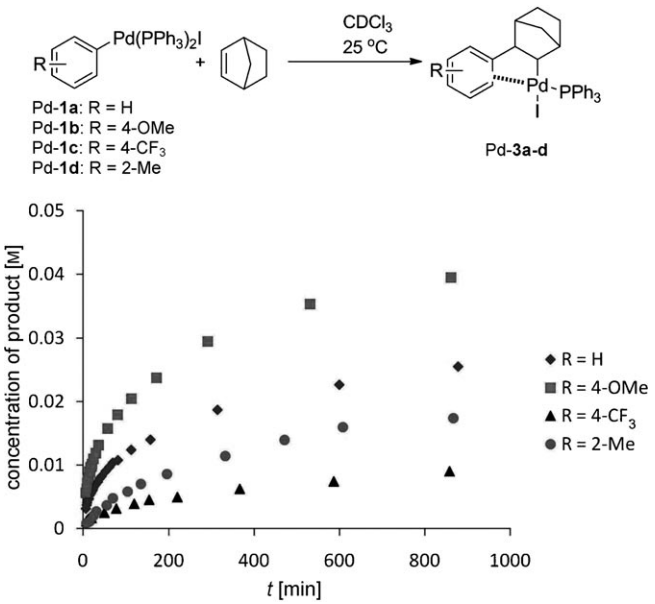

Figure 1. Comparison of rates of carbopalladation between Pd-**1a–d** and norbornene.

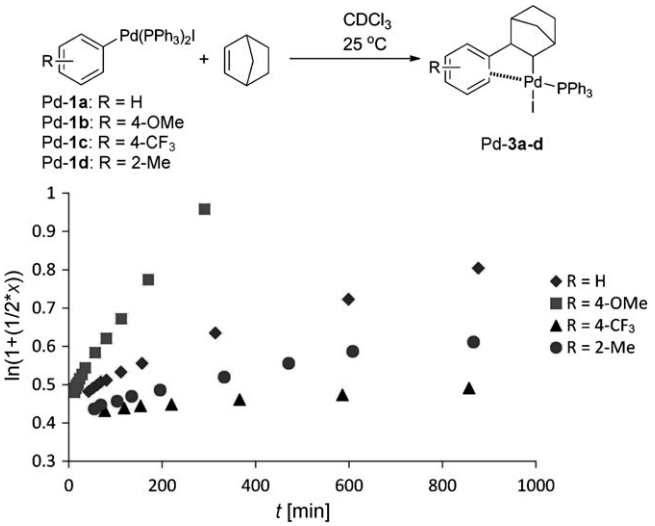

Figure 2. Linear relationship of $\ln(1+(1/(2\cdot x)))$ versus t [min] for carbopalladation of Pd-**1a–d** (42.9 mM) with norbornene (64.3 mM) in 0.7 mL of $CDCl_3$ at 25 °C; $x=[\text{Pd-}\mathbf{1}]_t/[\text{Pd-}\mathbf{1}]_0$; $k_{app}=0.0798\,\text{M}^{-1}\text{min}^{-1}$ (R = 4-OMe), $0.018\,\text{M}^{-1}\text{min}^{-1}$ (R = H), $0.0104\,\text{M}^{-1}\text{min}^{-1}$ (R = 2-Me), $0.00336\,\text{M}^{-1}\text{min}^{-1}$ (R = 4-CF_3).

electron-rich substituents favor carbopalladation. The reaction with sterically hindered Pd-**1d** ($k_{app}=0.0104\,\text{M}^{-1}\text{min}^{-1}$) occurred slower than that of the electron-neutral palladium complex, Pd-**1a**, but faster than that of the electron poor palladium complex Pd-**1c**.

Calculating those rate constants (k_{app}) at 25 °C, provided the following activation energies: $\Delta G^{\neq}=16.5\,\text{kcal mol}^{-1}$ (R = 4-OMe), $17.4\,\text{kcal mol}^{-1}$ (R = H), $18.4\,\text{kcal mol}^{-1}$ (R = CF_3), $17.7\,\text{kcal mol}^{-1}$ (R = 2-Me). These activation values are lower than the $23\,\text{kcal mol}^{-1}$ activation energy previously reported for the Heck reaction of iodobenzene and methyl acrylate in the presence of a $Pd(OAc)_2/PPh_3$ catalytic system,[7] suggesting that norbornene insertion is kinetically faster than the insertion of methyl acrylate. Indeed, a reaction of a mixture of aryl halide, alkene, and norbornene in the Catellani process shows that norbornene insertion is faster than alkene insertion unless the aryl halide exerts a large steric effect by the presence of two *ortho*-substituents.[8]

This observed electronic trend indicates that the migration of the aryl group from the palladium complex onto the alkene is viewed as a nucleophilic addition to the double bond. Two mechanisms are the most widely accepted in the Heck reaction:[9] the neutral mechanism, which is initiated by the dissociation of a phosphine ligand and subsequent association of an alkene,[9b] and the cationic mechanism, which is initiated by the dissociation of a halide ligand and subsequent association of an alkene.[9c] However, since the rate of carbopalladation was not largely affected by adding 1 equiv of Bu_4NI in our reaction, the cationic mechanism seems less likely in this case.

With the proposed intermediate Pd-**2** (Scheme 4), we sought to detect the intermediate by variable temperature NMR during the carbopalladation process.[10] Unfortunately, any possible intermediates could not be detected at a variety of temperatures presumably due to the fast migration of the aryl group to the double bond in norbornene (k_2 and/or $k_{-1} \gg k_1$).

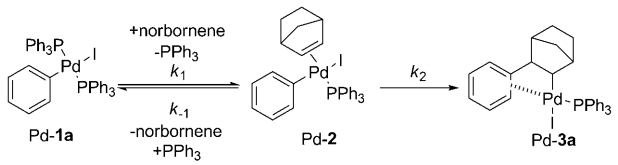

Scheme 4. Proposed mechanism of carbopalladation.

Kinetic order of the reaction: ***Step 1***: Next, we turned our attention to analyze the kinetic orders of Pd-**1**, norbornene, and PPh_3 to elucidate the proposed mechanism. We chose Pd-**1b** (R = 4-OMe) in this study due to easier spectroscopic analysis. Rate Equation (2) was derived for this study using the steady state approximation where k_1 and k_{-1} represent reversible ligand exchange and k_2 represents the carbopalladation step (see Supporting Information for the derivation). It is worth noting that Pd-**3** did not undergo retro-carbopalladation, even at 60 °C, both in the presence and absence of PPh_3 unless a large steric effect exerted by *ortho*-substituents results in destabilization of Pd-**3**.

We first examined the rate of the carbopalladation from Pd-**1b** by reacting norbornene (42.9 mM) and PPh_3

$$\text{rate} = \frac{k_1 k_2[\text{Pd-}\mathbf{1b}][\text{norbornene}]}{k_{-1}[\text{PPh}_3] + k_2} \qquad (2)$$

(21.4 mM) with varying Pd-**1b** concentration (21.4 mM to 85.7 mM) in $CDCl_3$ at 25 °C. The reaction was monitored by ^1H NMR, and the initial rate was determined at each concentration of Pd-**1b**. As described in Figure 3, the order in Pd-**1b** was determined to be first order, which is consistent with the rate equation involving a monomeric palladium species.

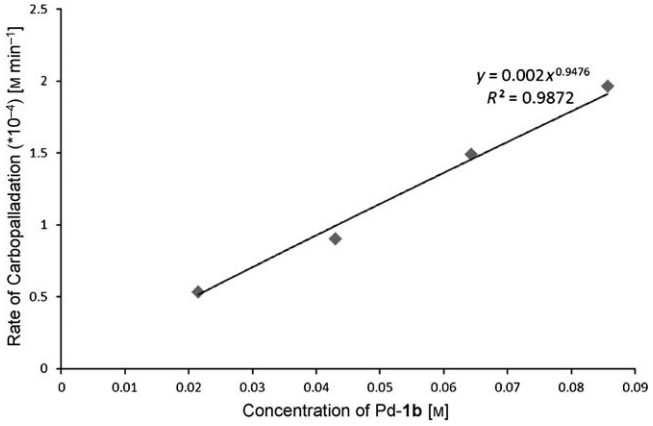

Figure 3. A plot of initial rate [M min^{-1}] vs concentration of Pd-**1b**: First-order dependence.

The order in norbornene was next determined by analogous procedure, using Pd-**1b** (42.9 mM), PPh_3 (21.4 mM), and varying norbornene concentration (21.4 mM to 85.7 mM) in $CDCl_3$ (Figure 4). As expected, a first order dependence in norbornene was observed.

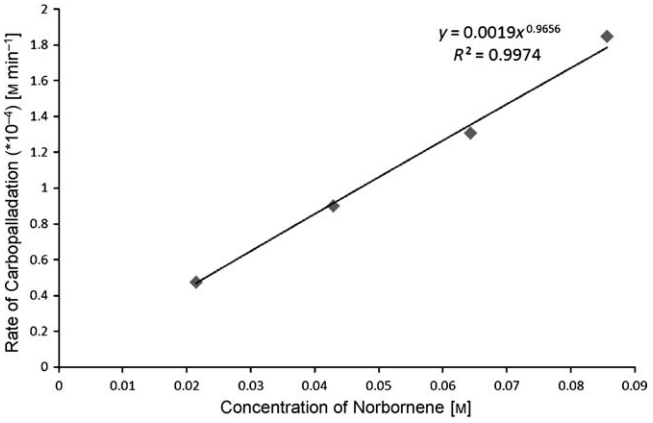

Figure 4. A plot of initial rate [M min^{-1}] vs concentration of norbornene: First-order dependence

Finally, the order of PPh_3 was examined using Pd-**1b** (42.9 mM), norbornene (42.9 mM), and varying the PPh_3 concentration (21.4 mM to 85.7 mM) (Figure 5). Qualitatively, the reaction rate decreased with increasing [PPh_3], suggesting an inverse order dependence on phosphine ligands. A nonlinear least-squares fit calculated from Excel function to the equation: $r = a[PPh_3]^n$ revealed an order n of −0.93,

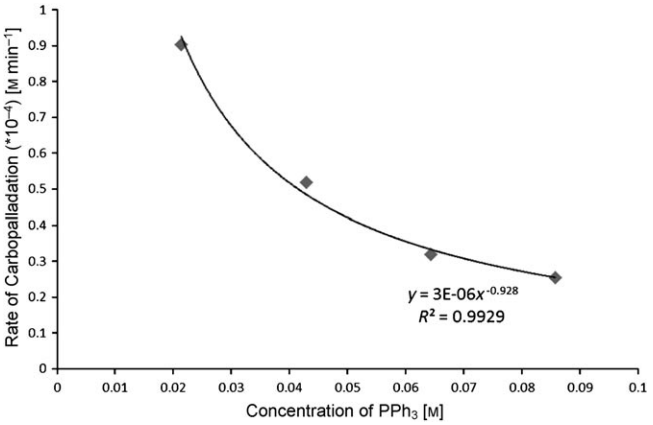

Figure 5. A plot of initial rate [M min^{-1}] vs. concentration of PPh_3: Inverse-order dependence.

which is only a slight deviation from an inverse first order due to k_2 value [$r \propto \{k_{-1}[PPh_3] + k_2\}^{-1}$, see Equation (2)].

Proposed mechanism of the carbopalladation: ***Step 1***: The close fit between experimental and predicted kinetic data allows us to support the proposed mechanism shown in Scheme 4. For example, Equation (2) predicts the reaction to be first order in Pd-**1b**, first order in norbornene, and inverse order in PPh_3, consistent with the experimental kinetic data. The reaction is first initiated by a reversible ligand exchange between the phosphine ligand and norbornene, then a subsequent carbopalladation to form Pd-**3a**.

X-ray crystal structure of complex Pd-3e: Pure palladium complex Pd-**3e** was synthesized from the corresponding aryl iodide and norbornene using [$Pd(PPh_3)_4$] in THF at 60 °C in good yields (see Scheme 6 below). A relatively fast crystallization was necessary due to the decomposition of the complex, which occurred during prolonged storage in solution at room temperature (~12 h). Crystals suitable for X-ray analysis were obtained in a few hours by dissolving Pd-**3e** in CH_2Cl_2 followed by the addition of MeOH.

The X-ray structure clearly shows that the aryl ring and the palladium are positioned *cis* and *exo* to the norbornyl group (Figure 6). The palladium possesses a slightly distorted square-planar center with the PPh_3, I^-, norbornyl group, and π-system of the aryl ring, in which the *ipso*-carbon (C8) of the π-system occupies one of the four coordination sites (14.3° dihedral angle between I-Pd-C8 and P-Pd-C1 planes). The *ortho*-carbon (C13) is out-of the plane (38.6° dihedral angle between I-Pd-C13 and P-Pd-C1 planes). The η^2 coordination to palladium can attribute to the longer bond length of C8–C13, which is measured to be 1.41 Å compared with 1.39 Å for the other aryl C–C bonds. In addition, the *ipso* carbon C8–Pd bond length is measured to be 2.42 Å, while C13–Pd has 2.52 Å, presumably due to stronger back-donation to C8 from palladium.[11] These bond lengths are slightly longer than previously reported η^2-alkene–palladium bonds.[12]

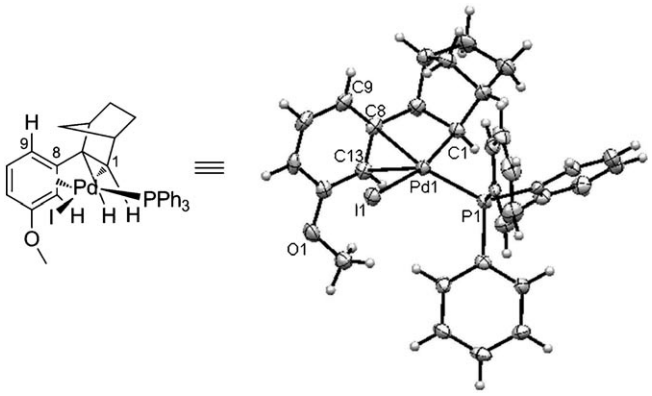

Figure 6. ORTEP structure of Pd-**3e** as determined by X-ray crystallographic characterization.

It is known that the dynamic NMR behavior of an analogous palladium complex results in a mixture of two isomers due to rotation of the aryl group.[6e] Interestingly, in solid state, the aryl group adapts a conformation in which the methoxy group is positioned near the palladium. It is worth noting that the H on C9 seems to experience more steric effect with the norbornyl group than the H on C13, which is positioned away from the norbornyl group (Figure 6). This assumption suggests that the complex possessing an *ortho*-substituted aryl group would adapt a structure such as Pd-**A** (Scheme 5). However, the conformation Pd-**B** should be a key for the C1–H functionalization leading to the palladacycle. Presumably, an equilibrium exists between these two structures in solution. A detailed structural analysis of this complex is on-going and will be published in due course.

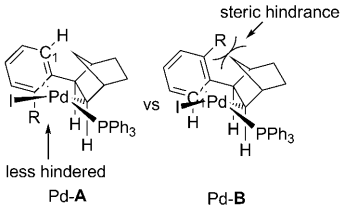

Scheme 5. Proposed structure of the 2-substituted phenyl norbornyl palladium complex.

NMR analysis of palladacycle formation: ***Step 2***: Pure palladium complexes Pd-**3a** and Pd-**3e** were synthesized from their corresponding aryl iodides and norbornene using [Pd(PPh_3)$_4$] in THF at 60 °C in good yields (Scheme 6). However, the electron-poor palladium complex Pd-**3f** could not be prepared by this one-step method due to poor stability of the product under the conditions. Since we had observed reaction between Pd-**1c** and norbornene in $CDCl_3$ by NMR, we thought to use this two-step method for the synthesis of Pd-**3f**. Indeed, these sequential reactions gave relatively pure complex Pd-**3f** in 80% yield, but with incomplete conversion.

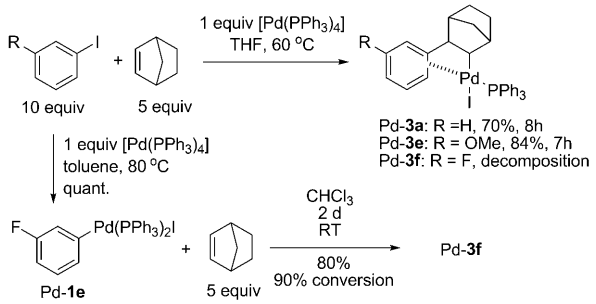

Scheme 6. Syntheses of norbornyl palladium complexes.

With the palladium complexes in hand, we next sought to probe the Hammett relationship to describe the rate acceleration by electronic effects in the C–H functionalization step. For this study, we switched the base from Bu_4NOH to KOPh to increase the reaction rate; full conversion was obtained in 5 days with Bu_4NOH compared to 30 min with KOPh. However, the instability of the electron-poor palladium complex Pd-**3f** and the large rate fluctuation without stirring in a NMR tube resulted in poor kinetic data (Table 3).

Table 3. Kinetic data for palladacycle formation via C–H functionalization.[a]

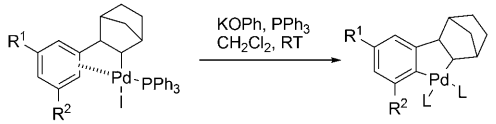

Pd-**3a**: R^1, R^2 =H
Pd-**3e**: R^1 = OMe, R^2 = H
Pd-**3f**: R^1 = F (or H), R^2 = H (or F)

Pd-**5a, e, f**

Entry	Substrate	Product	*t* [h]	Conversion [%][b]
1	Pd-**3a**	Pd-**5a**	0.5	67[c]
2	Pd-**3a**	Pd-**5a**	1	86[c]
3	Pd-**3e**	Pd-**5e**	0.5	67
4	Pd-**3e**	Pd-**5e**	1	86
5	Pd-**3f**	Pd-**5f**	0.5	100[d]

[a] Reactions were conducted with Pd-**3** (0.03 mmol), KOPh (0.09 mmol) and PPh_3 (0.054 mmol) in CH_2Cl_2 (2.0 mL). [b] Measured by ^1H NMR. [c] Small amount of decomposed products found. [d] Large amount of decomposition products found.

Thus, we turned our attention to NMR spectroscopic analysis for the detection of possible intermediates. ^{31}P NMR spectroscopic analysis of Pd-**3a** in $CDCl_3$ showed one singlet signal at 38.9 ppm (Figure 7a). This signal was broadened upon the addition of 1 equiv of PPh_3 at 25 °C, which could be a result of fast equilibrium between Pd-**3a** and a new palladium complex (Figure 7b). However, the resonances are sharpened to a single signal at low temperature (Figure 7d), suggesting that the phosphine ligand on Pd-**3a** exchanges with free phosphine at 25 °C, but not at –50 °C.

We next examined ^{31}P NMR of Pd-**3a** with KOPh in the absence of PPh_3 in $CDCl_3$ (Figure 8). When Pd-**3a** and excess KOPh were combined at –40 °C, a new broad peak

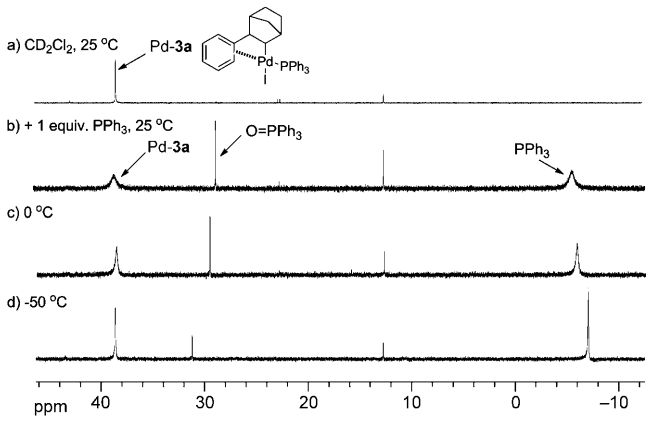

Figure 7. ^{31}P NMR study of reaction between Pd-**3a** (30 mM) and PPh_3 (60 mM) in $CDCl_3$. a) ^{31}P NMR of Pd-**3a** at 25 °C. b) ^{31}P NMR of Pd-**3a** taken at 10 min after addition of PPh_3 at 25 °C. c) ^{31}P NMR of Pd-**3a** taken at 10 min after cooling to 0 °C. d) ^{31}P NMR of Pd-**3a** taken at 10 min after cooling to −50 °C.

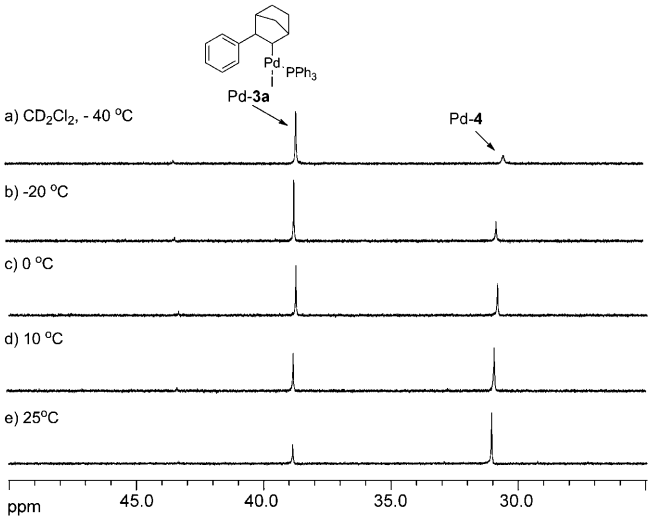

Figure 8. ^{31}P NMR study of reaction between Pd-**3a** (30 mM) and KOPh (150 mM) in CD_2Cl_2. a) ^{31}P NMR taken at 20 min after mixing of Pd-**3a** and KOPh in CD_2Cl_2 cooled in liquid nitrogen, −40 °C. b) ^{31}P NMR taken 10 min after warming to −20 °C. c) ^{31}P NMR taken 10 min after warming to 0 °C. d) ^{31}P NMR taken 10 min after warming to 10 °C. e) ^{31}P NMR taken 10 min after warming to 25 °C.

was observed at 30.7 ppm. Upon warming to 25 °C, this new signal grew to a 1:2.4 ratio corresponding to 70% conversion. Unfortunately, attempts to reach full conversion by increasing the amount of base, higher temperature, or increasing concentration of the reaction resulted in decomposition of this species, Pd-**4**.

A sample containing Pd-**4** and a small amount of Pd-**3** was treated with excess PPH_3 to follow its conversion to Pd-**5**. The reaction of the new complex Pd-**4** was investigated by ^{31}P NMR by subjecting excess PPh_3 in $CDCl_3$ to a mixture containing Pd-**4** and a small amount of Pd-**3a** at −50 °C (Figure 9). Some Pd-**5a** was present before the NMR experiment was started since it was necessary to warm up to at

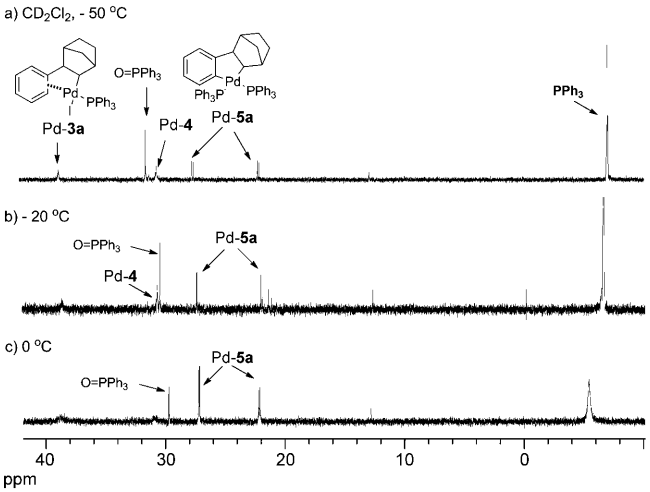

Figure 9. ^{31}P NMR study of reaction between Pd-**3a** (30 mM), KOPh (150 mM), and PPh_3 (60 mM) in $CDCl_3$. a) ^{31}P NMR taken at 20 min after mixing of Pd-**4** and PPh_3 in $CDCl_3$ cooled in liquid nitrogen, −50 °C. b) ^{31}P NMR taken at 10 min after warming to −20 °C. c) ^{31}P NMR taken at 10 min after warming to 0 °C.

least −20 °C to mix the reagents due to high viscosity. We believe that triphenylphosphine oxide was formed due to a small amount of water present in either Pd-**3a** or the solvent. The result showed an immediate transformation to the palladacycle Pd-**5a** upon warming up to 0 °C, with resonances appearing at δ 27.0 and 22.2 ppm as two sets of doublet with $J = 17.8$ Hz. On the basis of these NMR studies, we postulate that the new palladium complex Pd-**4** is a reactive species leading to the palladacycle Pd-**5a**.

Next we sought to deduce a structure of the new palladium complex Pd-**4**. In addition, incomplete conversion from Pd-**3** made structural determination difficult. Thus, the ^1H NMR of Pd-**4** formed in-situ from Pd-**3a** was analyzed at maximum conversion. This ^1H NMR corresponding to Pd-**4** shows a close match with one of Pd-**3a**, suggesting structural similarity (Figure 10).

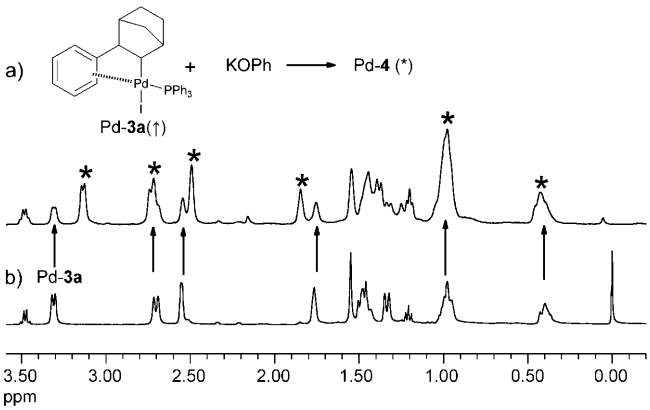

Figure 10. Comparison of ^1H NMR spectra of Pd-**4** and Pd-**3a** at −0.1 to 3.6 ppm. a) ^1H NMR of mixture of Pd-**4** and Pd-**3a** at maximum conversion, 70%. b) ^1H NMR of pure Pd-**3a**; * indicates peaks for Pd-**4** and ↑ indicates peaks for Pd-**3a**.

On the basis of these NMR studies, we postulate that Pd-**4** is an active palladium species, formed from Pd-**3a** by a ligand exchange between I^- and PhO^-, which undergoes the C–H functionalization to form the palladacycle Pd-**5a**.[13,14] Catellani suggested a similar ligand exchange process in her mechanistic study on the C–H functionalization of the norbornyl palladium complex with chloride and pyridine as ligands.[6a] In this report, she noted that the complex was stable at −50 °C, but underwent palladacycle formation at −30 °C with excess pyridine.

Kinetic isotope effect experiment of palladacycle formation: ***Step 2***: To further study the C–H functionalization process, we sought to measure the H/D kinetic isotope effect (KIE) for the deuterated substrates Pd-**3a**[D] and Pd-**3a**[D_5] [Eqs. (3) and (4)]. The Pd-**3a**[D] was synthesized from the palladacycle by treatment of DCl (see Section on reversibility of palladacycle for synthesis). No kinetic isotope effect was observed in the competition of Pd-**3a** and its pentadeuterated complex Pd-**3a**[D_5]. This suggests that the rate-limiting step does not involve C–H bond breakage. However, a primary isotope effect of 4.2 was determined from mono-*ortho*-deuterated complex Pd-**3a**[D]. In fact, this unusual KIE has been previously reported by Buchwald for the development of oxindole synthesis from α-chloroacetanilides via Pd-catalyzed C–H functionalization (Scheme 7).[15] In this report, he

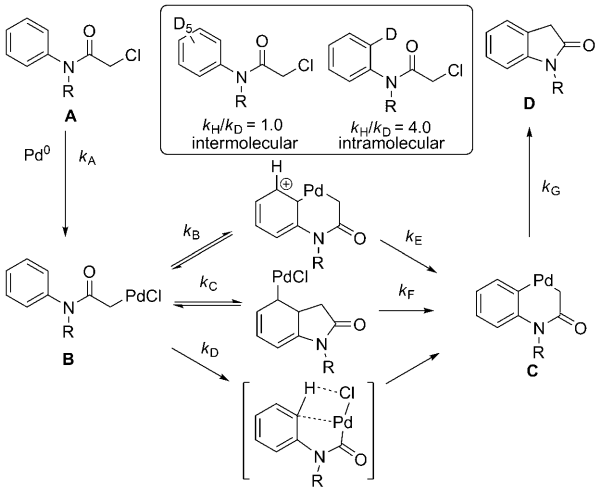

Scheme 7. Buchwald's palladium-catalyzed C–H functionalization for oxindole synthesis.[15]

suggested that the first oxidative addition (k_A) is slow relative to the C–H functionalization step and is rate-determining. This can explain the intermolecular KIE. Despite the rate-limiting oxidative addition, the alkyl palladium complex **B** can still choose either C–D bond or C–H bond breakage, resulting in a primary KIE. Then, the C–H functionalization step may proceed by either an electrophilic or a Heck-type mechanism if carbopalladation of the aromatic ring (k_B and k_C) is fast and reversible. Alternatively, a direct C–H bond activation may proceed. Those scenarios can rationalize the KIE observed.

Proposed mechanism of palladacycle formation: ***Step 2***: For palladium-catalyzed C–H functionalizations, several reaction pathways[17–20] have been proposed and, among those, electrophilic aromatic substitution and concerted metallation–deprotonation (CMD) are the most widely accepted. Comparatively, the oxidative C–H insertion process is rare in the absence of a directing group and Heck-like processes cannot provide the palladacycles such as Pd-**5a**.

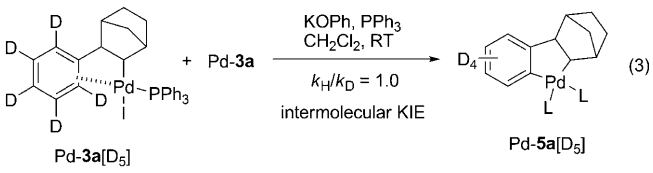

(3)

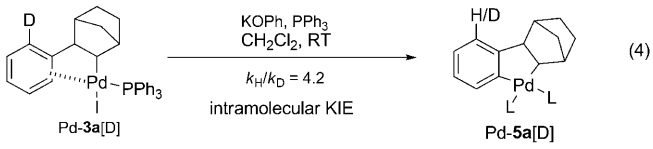

(4)

The data assembled for the palladacycle formation allow us to propose a mechanism. As shown in Scheme 8, the reaction is initiated by a ligand exchange, which seems to be a rate limiting step ($k_3 < k_4, k_6$) based on the observed kinetic isotope effect ($KIE_{inter} = 1.0$ and $KIE_{intra} = 4.2$). The C–H functionalization may proceed by an electrophilic aromatic substitution to give a cationic five-membered palladacycle, which is subsequently deprotonated to provide the palladacycle Pd-**5a**. The observed intramolecular KIE of 4.2 is reasonable if the k_4 step is reversible and fast relative to the deprotonation step. A second possible mechanism is a CMD-type mechanism via σ-metathesis or termolecular electrophilic (S_E3) mechanisms. Considering the slow ligand exchange step, this CMD mechanism also should explain the observed KIE values.

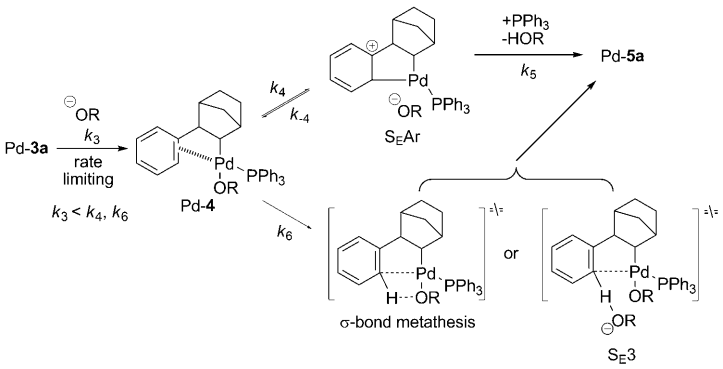

Scheme 8. Proposed mechanism of palladacycle formation.

X-ray crystal structure of Pd-5a: Single crystals suitable for X-ray analysis were obtained from a mixture of CH_2Cl_2 and MeOH. An ORTEP drawing of Pd-**5a** is shown in Figure 11. The palladium centre possesses square-planar geometry with dihedral angle of 7.98° between P2-Pd-C1 and P1-Pd-C13 planes. The bond lengths Pd–P1 and Pd–P2 are 2.41 and 2.38 Å, respectively.

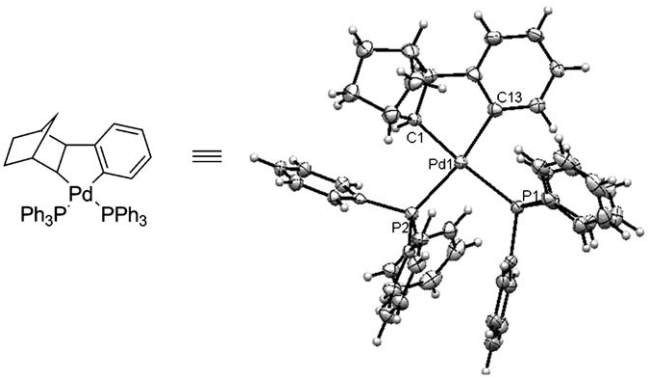

Figure 11. ORTEP structure of Pd-**5a** as determined by X-ray crystallographic characterization.

Reversibility of palladacycle: ***Step 2***: While we conducted the optimization study, we found an interesting reaction, suggesting the possibility for reversible palladacycle formation. The compound **16** was isolated in an H/D ratio of 1:1 when the reaction was performed under either the pyrrole annulation conditions (A) in the presence of 2 equiv D_2O or the benzocyclobutene reaction conditions (B) at 100 °C (Table 4, entries 2 and 5). However, no deuterium was incorporated when the reaction was conducted with CD_3OD at 100 °C (Table 4, entry 3). In fact, a stoichiometric reaction conducted under the anhydrous conditions (with Cs_2CO_3 as the base) revealed that the palladacycle was present in only trace amount. This result suggested that the palladacycle can only be formed with water present.[16] In addition, no deuterium was observed in **16** when the reaction was performed at 80 °C under both conditions (Table 4, entries 1 and 4), indicating that the reversibility only happens if sufficient energy is provided (i.e., >100 °C).

To further support this reversibility hypothesis, we conducted a reaction between the palladacycle Pd-**5a** and either D_2O or DCl [Eq. (5)]. The result showed that the palladacycle underwent a ring opening reaction with both D_2O and DCl, but in low conversion with D_2O (see Supporting Information for the detection of ring-opening product with D_2O). This result suggests that our biphasic and hydroxide-containing system for the benzocyclobutene reaction can reduce the rate of the ring-opening reaction by removing HI formed during the ring-closing reaction.

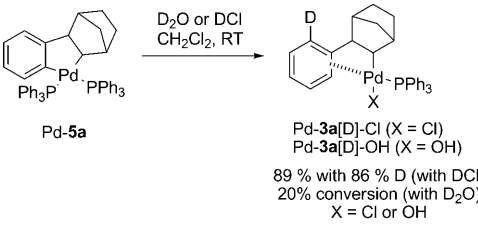

(5)

Table 4. Scope of benzocyclobutene reaction with aryl iodides and D_2O.[a]

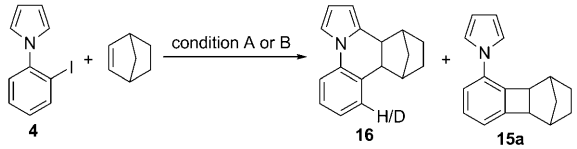

Entry	Conditions	T [°C]	**16** [%]	**15a** [%]
1	A	80	15 (no D)	0
2	A	100	45 (1:1 D/H)	0
3[b]	A	100	89 (no D)	0
4	B	80	5 (no D)	75
5	B	100	90 (1:1 D/H)	10

[a] Condition A: **4** (0.15 mmol), norbornene (0.6 mmol), 10 mol% $Pd(OAc)_2$, 22 mol% PPh_3, Cs_2CO_3 (0.3 mmol), toluene (1.5 mL), D_2O (0.3 mmol); condition B: **4** (0.15 mmol), norbornene (0.6 mmol), 10 mol% $Pd(OAc)_2$, 22 mol% PPh_3, KOD (0.3 mmol), toluene (0.5 mL), D_2O (0.5 mL); [b] with CD_3OD (0.3 mmol) instead of D_2O.

NMR analysis of reductive elimination: ***Step 3***: Since little or no reductive elimination occurred at temperatures lower than 70 °C in any solvent system, this study was conducted in [D_8]toluene at 80 °C. The palladacycle Pd-**5a** was only partially soluble below 60 °C, but became soluble at 80 °C.

The relative rate of the reductive elimination was unaffected by the addition of hydroxide or water, suggesting that this step occurs directly from the palladacycle. However, if the reaction was run at 40–60 °C in the absence of water, Pd-**5a** slowly decomposed to palladium black; whereas no decomposition was detected in the presence of water. Thus, it seems that even though water encourages palladacycle reversibility, it also increases the stability of the palladacycle.

In addition to Pd-**5a**, Pd-**5e** (R^1=OMe, R^2=H) was prepared to study electronic effects on the reductive elimination step. Surprisingly, Pd-**5e** did not produce the benzocyclobutene in [D_8]toluene at 80 °C, presumably because this electron-rich palladacycle is too stable. Indeed, the reactions using 4-iodoanisole under the optimized catalytic and stoichiometric reaction conditions did not provide corresponding benzocyclobutenes, even though the palladacycle was detected in the crude NMR analysis (see Section on the Scope of the reaction with other bicyclic systems and aryl halides for details).

Relatively fast reductive elimination at this temperature led to unreliable kinetic data. Thus, we studied this reaction by qualitative NMR analysis. However, no intermediates or by-products were detected in this study. Thus, we propose that the reductive elimination occurs directly from Pd-**5a**.

Unexpected new palladium complex: A few palladium(II) hydroxo-bridged dimers have been synthesized, character-

ized, and studied.[14] Experimentally, these complexes are usually prepared from an aryl halide by treatment of $[(PPh_3)_2PdCl_2]$ and KOH in biphasic conditions (benzene and water). In these reactions, the hydroxide ion serves two roles: to reduce Pd^{II} to Pd^0 and to act as a bridging ligand.[14d] Previous studies have demonstrated that the reduction process proceeds first by hydroxide-induced disproportionation of $[(PPh_3)_2Pd^{II}Cl_2]$ to highly reactive Pd^0PPh_3 and triphenylphosphine oxide. Then, oxidative addition of the aryl halide, followed by ligand exchange with hydroxide, results in the organopalladium hydroxo dimer $[\{(PPh_3)ArPd^{II}(\mu\text{-}OH)\}_2]$.

However, our attempts to synthesize this dimeric hydroxo palladium complex from 2-pyrrole substituted phenyl iodide resulted in isolation of an orange powder (50% yield), which clearly shows distinct patterns from the hydroxo-bridged dimers in ^1H NMR. Fortunately, a good quality crystal suitable for X-ray analysis could be obtained from CH_2Cl_2 and MeOH (Pd-**6**, Figure 12). The crystal structure

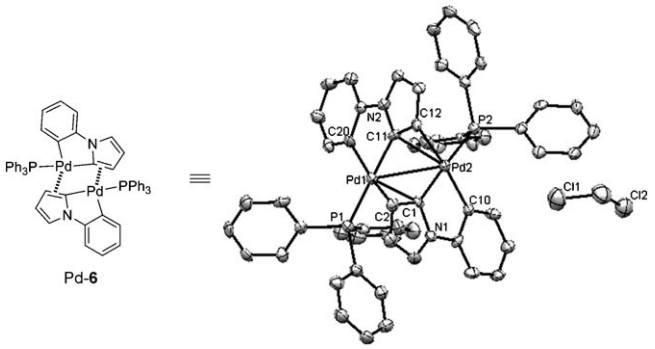

Figure 12. ORTEP structure of Pd-**6** as determined by X-ray crystallographic characterization.

consists of unusual dimeric units with the π-system of a pyrrole moiety acting as a bridging ligand. This dimer shows a slight deviation from C_2 symmetry with the Pd1–C1 and Pd1–C2 distances being 2.34 and 2.51 Å, respectively, and Pd2–C11 and Pd2–C12 distances being 2.38 and 2.55 Å, respectively. This difference attributes to a slightly shorter bond length for C11–C12 due to less π-electron contribution to palladium: 1.38 Å for C11–C12 versus 1.42 Å for C1–C2. In addition, the Pd1–Pd2 bond 2.86 Å is in a range of typical Pd–Pd bond lengths for known palladium dimers, 2.7–3.0 Å.[14,21]

Summary of mechanistic studies and proposed mechanism of benzocyclobutene formation: Our NMR studies to identify the palladium intermediates in the reactions of aryl halides with norbornene, together with kinetic studies for each reaction parameter, have shown that the reaction occurs through the Pd-**1**, Pd-**3**, Pd-**4**, and Pd-**5** intermediates as shown in Schemes 4 and 8. To establish a correlation between the reactions using 2-pyrrole substituted phenyl iodide **4a** and phenyl iodide, ^{31}P NMR data of **4a** under modified biphasic conditions (25 °C for two days) were obtained for both catalytic and stoichiometric reactions (see Supporting Information for NMR data). They clearly showed that complexes analogous to the previously identified norbornyl palladium complex Pd-**3** and palladacycle Pd-**5** were present. Moreover, a complex analogous to Pd-**5** was present as a major species. This result also suggests the reductive elimination step to be the rate-limiting step since no benzocyclobutene was obtained at 25 °C.

Both benzocyclobutene and pyrrole annulation reactions are initiated by oxidative addition of Pd^0[22] to aryl iodide to form the Pd^{II} complex Pd-**7** (Scheme 9). The oxidative addition is known to be slower in the presence of alkenes by formation of unreactive alkene–palladium complex $[Pd^0(norbornene)(PPh_3)_2]$.[23a] Then, a reversible ligand exchange with norbornene leads to Pd-**8**, followed by carbopalladation with norbornene to provide Pd-**9** according to the observed kinetic orders: first order to both palladium and norbornene and inverse order to the phosphine ligand. At this point, a ligand exchange between I^- and HO^- leads to Pd-**10**, as exemplified by an analogous alkoxide palladium complex Pd-**4** was observed by both ^1H and ^{31}P NMR. Subsequently, Pd-**10** undergoes a cyclization to give the five-membered palladacycle Pd-**11** via either electrophilic aromatic substitution or concerted metallation–deprotonation (CMD) mechanism based on the observed KIE. (KIE_{inter} = 1.0 and KIE_{intra} = 4.2). At this stage, the ligand exchange step was determined to be slower than the C–H functionalization step ($k_{10} < k_{11}$). A reductive elimination of Pd-**11** can occur to provide the benzocyclobutene **15**. However, if sufficient energy is provided (i.e., >100 °C), the reversibility be-

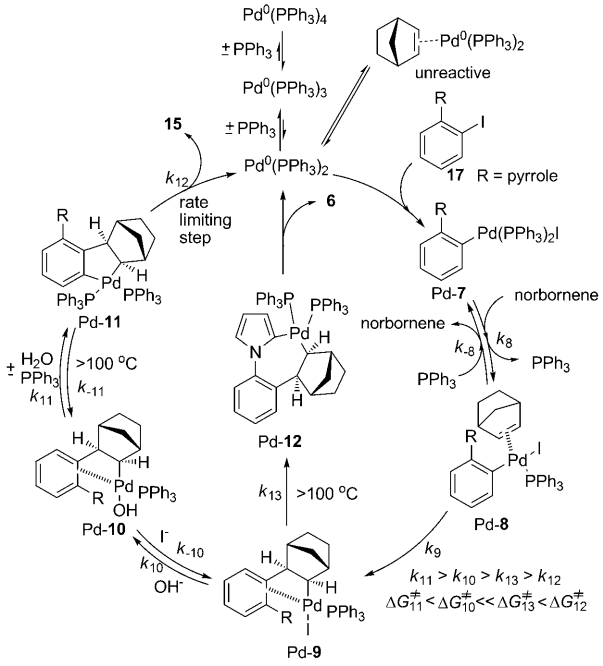

Scheme 9. Proposed mechanisms of benzocyclobutene and pyrrole annulation reactions based on mechanistic studies.

tween Pd-**11** and Pd-**9** allows fast equilibrium prior to a pyrrole C–H bond functionalization to afford the seven-membered palladacycle Pd-**12** ($k_{13} < k_{10}$). Then, Pd-**12** can undergo a reductive elimination to produce the pyrrole annulation product **6**. This mechanism can explain how the deuterium-labeled **16** was formed in an H/D ratio of 1:1 (Table 4, entry 5). The activation energy ($\Delta G_{13}^{\neq}$) toward the pyrrole annulation product **6** is lower than that ($\Delta G_{12}^{\neq}$) of benzocyclobutene **15**, thus favoring **6** under the equilibrium condition ($\Delta G_{13}^{\neq} < \Delta G_{12}^{\neq}$).

In case of the $Pd(OAc)_2/PPh_3$ catalytic system, we expect the mechanism to be more complex since it has been shown that acetate ions are crucial ligands to accelerate the rate-limiting carbopalladation step in the Heck reaction.[23]

Scope of the reaction with other bicyclic systems and aryl halides: With mechanistic data in hand, we sought to study the reactivity with numerous aryl halides and bicycle systems. Poor reactivity was expected with both electron poor and electron rich aryl halides due to the instability of electron poor palladacycles (see Table 3) and high stability of electron rich palladacycles (see Section on NMR analysis of reductive elimination: Step 3). As expected, both electron rich and poor aryl halides gave no reaction with the exception of 2-substituted aryl halides such as **18e** and **18h** (Table 5). It seems that the observed reactivity of **18e** and **18h** are primarily the result of steric influence of the substituent, increasing the rate of the reductive elimination by relief of steric strain. Attempts to increase the reaction temperature for unreactive substrates resulted in decomposition (Table 5, entries 6–7 and 9–11).

We next examined a variety of 2-pyrrole-substituted substrates, including electron-rich and -poor phenyl iodide **4**. In these cases, the benzocyclobutene could not be obtained, regardless of electronic effects (Table 6, entries 4–8). However, the reaction of electron-neutral aryl iodides **4a** resulted in high yield of the corresponding benzocyclobutene **15a** with excellent regioselectivity (Table 6, entry 1). The annulation reaction can also be extended to other bicyclic systems such as norbornadiene **20b** or benzonorbornadiene **20c** (Table 6, entries 2–3).

Table 5. Scope of benzocyclobutene reaction with aryl iodides.[a]

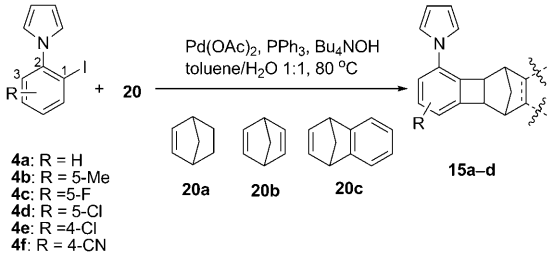

Entry	Substrate	R	Product	Yield [%][b]
1	**18a**	H	**19a**	quant.
2	**18b**	2-Me	**19b**	quant.
3	**18c**	2-Et	**19c**	quant
4	**18d**	2-*i*Pr	**19d**	90
5	**18e**	2-OMe	**19e**	90
6	**18f**	3-OMe	**19f**	NR[c]
7	**18g**	4-OMe	**19g**	NR[c]
8	**18h**	2-CF_3	**19h**	95
9	**18i**	3-CF_3	**19i**	NR[c]
10	**18j**	4-CF_3	**19j**	NR[c]
11	**18k**	3-Me	**19k**	30[c,d]

[a] Reactions were conducted with $Pd(OAc)_2$ (10 mol%), PPh_3 (22 mol%), Bu_4NOH (0.6 mmol), **18** (0.3 mmol), norbornene (1.2 mmol), toluene (1 mL), H_2O (1 mL). [b] Isolated yield. [c] Reactions at 100°C resulted in decomposition. [d] Isolated as two regioisomers.

Table 6. Scope of benzocyclobutene reaction with 2-pyrrole substituted aryl iodide.[a,b]

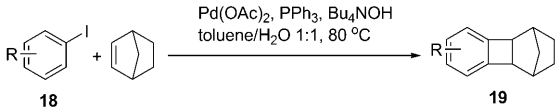

Entry	4	20	Product	Yield [%][c]
1	**4a**	**20a**	**15a**	95–100
2	**4a**	**20b**	**15b**	80
3	**4a**	**20c**	**15c**	50
4	**4b**	**20a**	**15d**	–[d,c]
5	**4c**	**20a**	**15e**	NR[e]
6	**4d**	**20a**	**15f**	NR[e]
7	**4e**	**20a**	**15g**	NR
8	**4f**	**20a**	**15h**	NR

[a] Reactions were conducted with $Pd(OAc)_2$ (10 mol%), PPh_3 (22 mol%), Bu_4NOH (0.6 mmol), **4** (0.3 mmol), **20** (1.2 mmol), toluene (1 mL), H_2O (1 mL). [b] Reactions with other bicyclic systems such as oxabicycle or azabicycle were not effective. [c] Isolated yield. [d] Reproducibility problems. [e] Reactions at 100°C resulted in pyrrole annulation.

Conclusion

In summary, we carried out detailed mechanistic investigations and a synthetic scope of Pd-catalyzed aryl C–H functionalization of phenyl iodides with strained alkenes. In this study, we have demonstrated that either benzocyclobutenes or pyrrole annulation products can be selectively synthesized from the reaction between 2-pyrrole phenyl iodide and norbornene at 80 or 100°C, respectively, in the presence of water and hydroxide ions. This mechanistic study provides the following insight into the factors that control the selectivity of both the pyrrole annulation and benzocyclobutene reactions: 1) Ligand exchange between I^- and HO^- is responsible for five-membered palladacycle formation, but this formation is reversible at higher temperature (>100°C). 2) Higher temperatures (>100°C) are required for pyrrole annulation, while benzocyclobutene formation can be selectively formed at low temperature (80°C). 3) The biphasic, basic conditions can slow down the reversible palladacycle by removing HX. This study also provides important features about the palladacycle formation: 1) The palladacycle only can be formed in the presence of water present in toluene.[16] 2) The palladacycle formation is reversible in the presence of water at >100°C, but irreversible at 80°C. Although this study does not explain the regioselectivity ob-

served in the original reaction conditions (MeCN and Cs_2CO_3, Scheme 2), we believe that there are common factors controlling the regioselectivity in these two reaction conditions ($MeCN/CO_3^{2-}$ vs toluene/H_2O/HO^-). Further study towards coupling of the palladacycle and alkyl halides or other oxidants is on-going and will be reported in due course. Additionally, the reactivity of the new palladium complex Pd-**6** is on-going and will be reported in due course.

Experimental Section

General method for synthesis of benzocyclobutenes 15 and 19: Aryl iodide **4** or **18** (0.15 mmol), $Pd(OAc)_2$ (10 mol%), and PPh_3 (22 mol%) were dissolved in toluene (0.5 mL) in a tapered microwave vial. To this mixture was added norbornene or bicyclic derivatives (0.6 mmol) in one portion. Then, Bu_4NOH (0.2 mL, 40 wt% in H_2O, 2 equiv) and water (0.3 mL) were immediately added via syringe, sealed, then heated to 80°C for 12 h in a pre-heated oil bath. Once cooled, the mixture was diluted with ether (0.5 mL) and water (0.5 mL) and extracted with diethyl ether (3×1 mL). The combined organic layers were then dried ($MgSO_4$), filtered, and the solvent removed in vacuo to yield the crude pyrrole. The crude material was purified by column chromatography.

Annulation product 15a: Purified by flash column chromatography (hexane/dichloromethane 6:1) yielding the title compound as a white solid (34.9 mg, 99%). M.p. 63–64°C; ^{1}H NMR (400 MHz, C_6D_6): δ = 7.27–7.20 (m, 4H), 6.83–6.81 (m, 1H), 6.32 (t, 2H; J=2.19 Hz), 3.37 (d, 1H; J=3.86 Hz), 3.21 (d, 1H; J=3.84 Hz), 2.41 (dd, 1H; J=3.04 & 1.35 Hz), 2.31 (dd, 1H; J=3.00 & 1.32 Hz), 1.65–1.59 (m, 2H), 1.25–1.20 (m, 2H), 1.03–0.94 ppm (m, 2H); ^{13}C NMR (100 MHz, C_6D_6): δ = 148.3, 134.2, 133.9, 128.9, 118.8, 118.4, 116.2, 110.2, 50.7, 50.2, 36.6, 36.2, 32.1, 27.8, 27.7 pppm; IR ($CHCl_3$): ν_{max} = 2951 (s), 2869 (w), 1600 (m), 1500 (s), 1338 (m), 1078 (m), 773 (m), 723 cm^{-1} (m); ESI MS: m/z: calcd for $C_{17}H_{18}N$ 236.1443: found 236.1427 $[M+H]^+$.

General procedure for synthesis of norbornyl palladium complex: In a sealable round-bottom flask containing $[Pd(PPh_3)_4]$ (1 mmol) and THF (20 mL) was added the aryl halide (10 mmol) via syringe. After flushing with argon for at least 10 min, norbornene (7 mmol) was added as a solid in one portion, sealed, and heated to 60°C for 8 h. After cooling down to room temperature, solvent was removed under reduced pressure and the residue was redissolved in diethyl ether (7 mL). The product slowly precipitated out by scratching. The product was collected by filtration and washed with small amount of ether (2×3 mL). Recrystallized from CH_2Cl_2 + MeOH if necessary.

[Ph(C_6H_{10})Pd(PPh_3)I] (Pd-3a): Synthesized according to the general procedure using phenyl iodide. Isolated as orange solid. Yield: 70% (45% after recrystallization); m.p. 145–150°C (decomp); ^{1}H NMR (400 MHz, $CDCl_3$): δ = 7.95 (brs, 2H), 7.70 (t, 6H; J=7.6 Hz), 7.56 (m, 3H), 7.44–7.35 (m, 9H), 3.31 (d, 1H; J=7.6 Hz), 2.70 (d, 1H; J=10 Hz), 2.55 (d. 1H; J=2.4 Hz), 1.77 (s, 1H), 1.51–1.43 (m, 2H), 1.33 (d, 1H; J= 10 Hz), 1.03–0.90 (m, 2H), 0.43–0.33 ppm (m, 1H); ^{13}C NMR (100 MHz, $CDCl_3$): δ = 135.2, 135.1, 135.0, 134.9, 131.9, 131.8, 131.4, 131.0, 130.5, 130.5, 130.1, 128.9 (br), 128.1, 128.0, 127.6 (m), 103.0, 102.9, 54.6, 54.5, 43.8, 43.7, 42.8, 42.6, 40.3, 37.8, 29.9, 29.8, 27.8 ppm; ^{31}P NMR (161 MHz, $CDCl_3$): δ = 38.8; ESI MS: m/z: calcd for $C_{31}H_{30}$PPd: 539.1114: found 539.1094 $[M-I]^+$.

[Ph[D_1](C_6H_{10})Pd(PPh_3)Cl] (Pd-3a[D]-Cl): Synthesized according to the Echavarren's procedure.[24] To a vial containing AcCl (5 mmol) was added deuterated methanol (5 mmol) dropwise at 0°C and stirred at this temperature for 30 min. To a 100 mL round-bottom flask containing the palladacycle (1 mmol) in CH_2Cl_2 (34 mL per Pd mmol) was added D-Cl solution (4.14 mL per Pd mmol) and stirred at ambient temperature for 3.5 h. The solvent was removed by vacuum and dilute with diethyl ether (7 mL). The precipitates formed were collected by filtration. Yield: 89% (with 74% D). M.p. 150–160°C (decomp); ^{1}H NMR (400 MHz, CD_2Cl_2): δ = 7.88 (d, 1.26H; J=6.8 Hz), 7.55 (dd, 6H; J=11.6, 7.2 Hz), 7.41–7.48 (m, 3H), 7.37–7.29 (m, 9H), 3.21 (d, 1H; J=7.2 Hz), 2.60, (d, 1H; J= 9.6 Hz), 2.44 (d, 1H; J=2.0 Hz), 1.45 (brs, 1H), 1.40–1.38 (m, 1H), 1.25 (d, 1H; J=10.0 Hz), 1.18 (t, 1H; J=8.8 Hz), 0.94–0.86 (m, 2H), 0.32 ppm (m, 1H); ^{13}C NMR (100 MHz, CD_2Cl_2): δ = 135.0, 134.9, 134.8, 134.8, 134.7, 134.6, 131.9, 131.8, 131.5, 131.3, 130.8, 130.7, 130.6, 130.5, 130.4, 128.4, 128.3, 128.2, 128.2, 128.1, 128.0, 127.9, 127.9, 127.7, 127.6, 54.2, 43.0, 42.9, 40.7, 38.2, 36.9, 36.8, 29.7, 29.6, 29.5, 28.0, 15.0 ppm; ^{31}P NMR (161 MHz, $CDCl_3$): δ = 35.5 ppm; ESI MS: m/z: calcd for $C_{31}H_{29}$DPPd: 540.1177: found 540.1161 $[M-I]^+$.

[Ph[D_1](C_6H_{10})Pd(PPh_3)Cl] (Pd-3a[D]): Pd-**3a**[D_1]-Cl (1 mmol) was treated with KI (5 mmol) in CH_2Cl_2 (33.3 mL mmol^{-1}) and stirred overnight at room temperature. The mixture was washed with water (3× 10 mL) and the organic layer dried over Na_2SO_4, and filtered. After the solvent was evaporated under vacuum, the residue was treated with ether, and the precipitates were collected by filtration. Yield: 75% (78%D). M.p. 148–155°C (decomp); ^{1}H NMR (200 MHz, CD_2Cl_2): δ = 7.96 (m, 1.22), 7.63–7.64 (m, 6H), 7.56 (m, 3H), 7.44–7.35 (m, 9H), 3.30 (d, 1H; J=7.6 Hz), 2.73 (d, 1H; J=10.0 Hz), 2.55 (d, 1H; J=3.6 Hz), 1.76 (s, 1H), 1.55–1.30 (m, 3H), 1.06–0.88 (m, 2H; 0.47–0.31 ppm (m, 1H); ^{13}C NMR (100 MHz, CD_2Cl_2): δ = 137.1, 137.0, 136.9, 136.9, 136.8, 136.7, 136.6, 136.5, 133.9, 133.5, 133.4, 132.7, 132.5, 132.4, 132.3, 132.1, 131.4, 130.8, 130.8, 130.7, 130.7, 129.9, 129.8, 129.8, 129.5, 129.5, 129.4, 129.4, 129.3, 56.5, 56.4, 45.8, 45.7, 45.0, 44.9, 42.3, 39.6, 31.7, 31.6, 31.5, 29.6 ppm; ^{31}P NMR (81 MHz, CD_2Cl_2): δ = 38.9; ESI MS: m/z: calcd for $C_{31}H_{29}$DPPd: 540.1177: found 540.1153 $[M]^+$.

General procedure for synthesis of palladacycles (Pd-5): A sealable round-bottom flask containing norbornyl palladium complex, Pd-**3** (0.5 mmol), KOPh (1.5 mmol), and PPh_3 (0.9 mmol) was flushed with argon for at least 10 min. Then, CH_2Cl_2 (67 mL mmol^{-1}) was added, sealed, and stirred for 1 h. After this time, the reaction was quenched by adding H_2O (12 mL mmol^{-1}) and the organic layer was washed with water (3×10 mL). The combined extracts were dried over Na_2SO_4, filtered, and solvent was removed under reduced pressure. The residue was redissolved in diethyl ether (7 mL). The product slowly precipitated out by scratching at cold temperature. The product was collected by filtration and washed with small amount of cold ether (2×3 mL) and cold acetone (2×2 mL). Recrystallized from CH_2Cl_2 + MeOH if necessary.

[{C_6H_4}C_6H_{10}Pd(PPh_3)$_2$] (Pd-5a): Synthesized according to the general procedure. Isolated as off-white solid. Yield: 70%. M.p. 105–110°C (decomp); ^{1}H NMR (400 MHz, CD_2Cl_2): δ = 7.73 (t, 6H; J=8.8 Hz), 7.53 (t, 6H; J=8.8 Hz), 7.46 (dt, 3H; J=7.2, 1.2 Hz), 7.44–7.30 (m, 9H), 7.23 (t, 6H; J=6.8 Hz), 7.10 (d, 1H; J=7.6 Hz), 6.83 (m, 2H), 6.32 (t, 1H; J=7.6 Hz), 3.18 (s, 1H), 2.90 (dd, 1H; J=14.8, 7.2 Hz), 2.43 (s, 1H), 2.27 (t, 2H; J=8.8 Hz), 1.47 (m, 1H), 1.12 (m, 3H), 0.03 ppm (m, 1H); ^{13}P NMR (100 MHz, CD_2Cl_2): δ = 170.7, 170.6, 141.7, 141.6, 141.5, 141.4, 135.2, 135.1, 134.9, 134.8, 134.7, 134.5, 134.2, 133.9, 129.5, 129.4, 129.1, 127.9, 127.8, 127.4, 127.3, 122.7, 122.2, 122.1, 122.0, 121.9, 121.8, 121.7, 66.9, 66.8, 66.1, 66.0, 64.0, 63.9, 48.0, 44.5, 44.4, 34.8, 32.1, 32.0, 32.0, 31.9, 30.5, 28.5 ppm; ^{31}P NMR (161 MHz, CD_2Cl_2): δ = 27.2 (d, J=17.8 Hz), 22.3 ppm (d, J=17.8 Hz); ESI MS: m/z: calcd for $C_{31}H_{30}$PPd: 539.1114: found 539.1138 $[M+H-PPh_3]^+$.

General procedure for synthesis of new palladacycle (Pd-6): A sealable round-bottom flask containing aryl halide **4** (1.2 mmol) and $[PdCl_2(PPh_3)_2]$ (1 mmol) was flushed with argon for at least 10 min. Then, benzene (14 mL) and aq. KOH (2.86 g KOH in 3 mL H_2O) were injected in sequence and refluxed for 3 h. After cooling to room temperature, the organic layer was washed with water (3×5 mL), and the extracts were dried over Na_2SO_4. After filtration, the solvent was removed under reduced pressure and the residue was redissolved in acetone (7 mL). The product slowly precipitated out by scratching. The product was collected by filtration and washed with small amount of cold acetone (2×3 mL) and cold acetone (2×2 mL). M.p. 150–155°C (decomp); ^{1}H NMR (400 MHz, $CDCl_3$): δ = 7.28 (m, 6H), 7.17 (t, 3H; J=7.2 Hz), 7.05 (d, 1H; J=3.2 Hz), 7.00 (dt, 6H; J=7.6, 1.6 Hz), 6.69 (t, 1H; J=7.6 Hz), 6.5–6.45 (m, 2H), 6.12 (dt, 1H; J=7.6, 1.2 Hz), 5.90 (m, 1H), 5.34 ppm (q, 1H; J=2.8 Hz); ^{13}C NMR (100 MHz, $CDCl_3$): δ = 206.9, 150.7,

144.2, 144.1, 140.3, 139.2, 139.1, 139.0, 135.5, 135.4, 132.1, 131.7, 129.4, 129.4, 127.6, 127.6, 127.5, 124.0, 123.8, 123.7, 121.4, 121.4, 110.5, 107.8, 107.8, 103.9, 103.9 ppm; ^{31}P NMR (121 MHz, $CDCl_3$): $\delta = 33.6$ ppm; ESI MS: *m*/*z*: calcd for $C_{28}H_{23}NPPd$: 510.0597.: found 510.0582 [*M*/2, monomeric].

Acknowledgements

We thank the Natural Science and Engineering Research Council of Canada (NSERC), the Merck Frosst Centre for Therapeutic Research, and the University of Toronto for funding. We thank Dr. Anny Jutand (CNRS) and Prof. Mark Taylor (University of Toronto) for helpful suggestions and comments. We also thank Dr. Alan Lough for X-ray crystallography analysis and Dr. Tim Burrow for variable temperature NMR studies. P.T. thanks NSERC for postgraduate scholarship (CGSM and CGSD).

[1] For a recent review, see: a) D. Alberico, M. E. Scott, M. Lautens, *Chem. Rev.* **2007**, 107, 174; b) P. Thansandote, M. Lautens, *Chem. Eur. J.* **2009**, *15*, 5874; c) G. P. Chiusoli, M. Catellani, M. Costa, E. Motti, N. Della Ca′, G. Maestri, *Coord. Chem. Rev.* **2010**, *254*, 456; d) F. Bellina, R. Rossi, *Tetrahedron* **2009**, *65*, 10269.

[2] a) M. Catellani, F. Frignani, A. Rangoni, *Angew. Chem.* **1997**, *109*, 142; *Angew. Chem. Int. Ed. Engl.* **1997**, *36*, 119; b) M. Lautens, S. Piguel, *Angew. Chem.* **2000**, *112*, 1087; *Angew. Chem. Int. Ed.* **2000**, *39*, 1045; c) M. Lautens, J. F. Paquin, S. Piguel, *J. Org. Chem.* **2002**, *67*, 3972; d) D. Alberico, J. F. Paquin, M. Lautens, *Tetrahedron* **2005**, *61*, 6283; e) C. Blaszykowski, E. Aktoudianakis, D. Alberico, C. Bressy, D. G. Hulcoop, F. Jafarpour, A. Joushaghani, B. Laleu, M. Lautens, *J. Org. Chem.* **2008**, *73*, 1888; f) T. Wilhelm, M. Lautens, *Org. Lett.* **2005**, *7*, 4053; g) A. Martins, M. Lautens, *Org. Lett.* **2008**, *10*, 5095; h) A. Rudolph, N. Rackelmann, M. Lautens, *Angew. Chem.* **2007**, *119*, 1507; *Angew. Chem. Int. Ed.* **2007**, *46*, 1485; i) A. Rudolph, N. Rackelmann, M. O. Turcotte-Savard, M. Lautens, *J. Org. Chem.* **2009**, *74*, 289; j) B. Mariampillai, J. Alliot, M. Li, M. Lautens, *J. Am. Chem. Soc.* **2007**, *129*, 15372; k) P. Thansandote, M. Raemy, A. Rudolph, M. Lautens, *Org. Lett.* **2007**, *9*, 5255; l) K. M. Gericke, D. I. Chai, M. Lautens, *Tetrahedron* **2008**, *64*, 6002; m) K. M. Gericke, D. I. Chai, N. Bieler, M. Lautens, *Angew. Chem.* **2009**, *121*, 1475; *Angew. Chem. Int. Ed.* **2009**, *48*, 1447; n) P. Thansandote, E. Chong, K.-O. Feldmann, M. Lautens, *J. Org. Chem.* **2010**, *75*, 3495; o) D. A. Candito, M. Lautens, *Angew. Chem.* **2009**, *121*, 6841; *Angew. Chem. Int. Ed.* **2009**, *48*, 6713.

[3] a) M. Catellani, *Top. Organomet. Chem.* **2005**, *14*, 174; b) M. Catellani, L. Ferioli, *Synthesis* **1996**, 769.

[4] For annulation onto an alkene, see: a) R. Grigg, P. Kennewell, A. Teasdale, V. Sridharan, *Tetrahedron Lett.* **1993**, *34*, 153. For annulation onto a nitrile, see: b) A. A. Pletnev, Q. Tian, R. C. Larock, *J. Org. Chem.* **2002**, *67*, 9276. For annulation onto phenols and anilines, see: c) M. Catellani, A. Del Rio, *Russ. Chem. Bull.* **1998**, *47*, 928; d) K. Saito, O. Katsuhiko, M. Sano, S. Kiso, T. Takeda, *Heterocycles* **2002**, *57*, 1781; e) M. Lautens, J.-F. Paquin, S. Piguel, M. Dahlmann, *J. Org. Chem.* **2001**, *66*, 8127; f) P. Thansandote, D. G. Hulcoop, M. Langer, M. Lautens, *J. Org. Chem.* **2009**, *74*, 1673.

[5] D. G. Hulcoop, M. Lautens, *Org. Lett.* **2007**, *9*, 1761.

[6] a) M. Catellani, G. P. Chiusoli, *J. Organomet. Chem.* **1992**, *425*, 151; b) M. Catellani, C. Mealli, E. Motti, P. Paoli, E. Perez-Carreno, P. S. Pregosin, *J. Am. Chem. Soc.* **2002**, *124*, 4336; c) C. Amatore, M. Catellani, S. Deledda, A. Jutand, E. Motti, *Organometallics* **2008**, *27*, 4549; d) C.-S. Li, C.-H. Cheng, F.-L. Liao, S.-L. Wang, *J. Chem. Soc. Chem. Commun.* **1991**, 710; e) C.-S. Li, D.-C. Jou, C.-H. Cheng, *Organometallics* **1993**, *12*, 3945; f) C.-H. Liu, C-S. Li, C.-H. Cheng, *Organometallics* **1994**, *13*, 18.

[7] F.-G. Zhao, B. M. Bhanage, M. Shirai, M. Arai, *Stud. Surf. Sci. Catal.* **1999**, *122*, 427.

[8] a) For intermolecular competition between Heck reaction and norbornene carbopalladation, see a) F. Jafarpour, M. Lautens, *Org. Lett.* **2006**, *8*, 3601. For intramolecular competition between Heck reaction and norbornene carbopalladation, see b) A. Martins, U. Marquardt, N. Kasravi, D. Alberico, M. Lautens, *J. Org. Chem.* **2006**, *71*, 4937.

[9] a) I. P. Beletskaya, A. V. Cheprakov, *Chem. Rev.* **2000**, *100*, 3009; b) C. Amatore, A. Jutand, *J. Organomet. Chem.* **1999**, *576*, 254; c) W. Cabri, I. Candiani, S. DeBarnardis, F. Francalanci, S. Penco, *J. Org. Chem.* **1991**, *56*, 5796.

[10] For observation of Pd^{II} alkene complexes, see a) P. S. Hanley, D. Markovic, J. F. Hartwig, *J. Am. Chem. Soc.* **2010**, *132*, 6302; b) C. S. Shultz, J. Ledford, J. M. DeSimone, M. Brookhart, *J. Am. Chem. Soc.* **2000**, *122*, 6351; c) F. C. Rix, M. Brookhart, *J. Am. Chem. Soc.* **1995**, *117*, 1137.

[11] C.-C. Huang, J.-P. Duan, M.-Y. Wu, F.-L. Liao, S.-L. Wang, C.-H. Cheng, *Organometallics* **1998**, *17*, 676.

[12] a) A. Segnitz, P. M. Bailev, P. M. Maitlis, *J. Chem. Soc. Chem. Commun.* **1973**, 698; b) M. F. Rettig, R. M. Wing, G. R. Wiger, *J. Am. Chem. Soc.* **1981**, *103*, 2980.

[13] For alkoxo-palladium(II) complexes, see a) M. Tanabe, K. Mutou, N. Mintcheva, K. Osakada, *Organometallics* **2008**, *27*, 519; b) E. Drent, J. A. M. van Broekhoven, M. J. Doyle, *J. Organomet. Chem.* **1991**, *417*, 235; c) E. Drent, P. Arnoldy, P. H. M. Budzelaar, *J. Organomet. Chem.* **1994**, *475*, 57; d) Y.-J. Kim, K. Osakada, A. Takenaka, A. Yamamoto, *J. Am. Chem. Soc.* **1990**, *112*, 1096; e) G. M. Kapteijn, A. Dervisi, D. M. Grove, H. Kooijman, M. T. Lakin, A. L. Spek, G. van Koten, *J. Am. Chem. Soc.* **1995**, *117*, 10939.

[14] The hydroxo–palladium complexes play an important role as synthetic precursors. For examples of dimeric hydroxo–palladium complexes, see: a) S. Kannan, A. J. James, P. R. Sharp, *Polyhedron* **2000**, *19*, 155; b) R. Schnebeck, E. Freisinger, B. Lippert, *Eur. J. Inorg. Chem.* **2000**, 1193; c) G. Pieri, M. Pasquali, P. Leoni, U. Englert, *J. Organomet. Chem.* **1995**, *491*, 27; d) V. V. Grushin, H. Alper, *Organometallics* **1993**, *12*, 1890; e) M. S. Driver, J. F. Hartwig, *Organometallics* **1997**, *16*, 5706; f) N. J. Ruiz, J. Cutillas, G. Samperdo, J. A. López, M. Hermoso, Martínez-Ripoll, *J. Organomet. Chem.* **1996**, *526*, 67; g) V. F. Kuznetsov, C. Bensimon, G. A. Facey, V. V. Grushin, H. Alper, *Organometallics* **1997**, *16*, 97. For examples of monomeric hydroxo-palladium complexes, see h) E. Alvaro, J. F. Hartwig, *J. Am. Chem. Soc.* **2009**, *131*, 7858; i) M. Akita, T. Miyaji, N. Muroga, C. Mock-Knoblauch, W. Adam, S. Hikichi, Y. Moro-oka, *Inorg. Chem.* **2000**, *39*, 2096; j) J. Cámpora, P. Palma, D. del Rio, E. Alvarez, *Organometallics* **2004**, *23*, 1652.

[15] For similar kinetic isotope effect in aromatic palladation reactions, see E. J. Hennessy, S. L. Buchwald, *J. Am. Chem. Soc.* **2003**, *125*, 12084 ($k_H/k_D = 4$ for intramolecular KIE; $k_H/k_D = 1$ for intermolecular KIE).

[16] We believe that water is not responsible for the palladacycle formation, but a small amount of hydroxide generated in-situ from water may undergo a ligand exchange with a halide on the palladium complex, which then undergoes the palladacycle formation.

[17] For palladium-catalyzed oxidative C–H insertion, see T. Okazawa, T. Satoh, M. Miura, M. Nomura, *J. Am. Chem. Soc.* **2002**, *124*, 5286.

[18] For palladium-catalyzed electrophilic C–H functionalization mechanism, see a) S. Pivsa-Art, T. Satoh, Y. Kawamura, M. Miura, M. Nomura, *Bull. Chem. Soc. Jpn.* **1998**, *71*, 467; b) B. S. Lane, M. A. Brown, D. Sames, *J. Am. Chem. Soc.* **2005**, *127*, 8050; c) C.-H. Park, V. Ryabova, I. V. Seregin, A. W. Sromek, V. Gevorgyan, *Org. Lett.* **2004**, *6*, 1159.

[19] For palladium-catalyzed Heck-like C–H functionalization process, see B. Glover, K. A. Harvey, B. Liu, M. J. Sharp, M. Tymoschenko, *Org. Lett.* **2003**, *5*, 301.

[20] For palladium-catalyzed CMD C–H functionalization process, see a) D. García-Cuadrado, P. de Mendoza, A. A. C. Braga, F. Maseras, A. M. Echavarren, *J. Am. Chem. Soc.* **2007**, *129*, 6880; b) D. L. Davies, S. M. A. Donald, O. Al-Duaij, S. A. Macgregor, M. Polleth, *J. Am. Chem. Soc.* **2006**, *128*, 4210; c) S. I. Gorelsky, D. Lapointe, K. Fagnou, *J. Am. Chem. Soc.* **2008**, *130*, 10848; d) B. Biswas, M. Sugi-

moto, S. Sakaki, *Organometallics* **2000**, *19*, 3895; e) D. L. Davies, S. M. A. Donald, S. A. Macgregor, *J. Am. Chem. Soc.* **2005**, *127*, 13754; f) D. García-Cuadrado, A. A. C. Braga, F. Maseras, A. M. Echavarren, *J. Am. Chem. Soc.* **2006**, *128*, 1066; g) M. Lafrance, C. N. Rowley, T. K. Woo, K. Fagnou, *J. Am. Chem. Soc.* **2006**, *128*, 8754; h) I. Alonso, M. Alcami, P. Mauleon, J. C. Carretero, *Chem. Eur. J.* **2006**, *12*, 4576; i) S. Pascual, P. de Mendoza, A. A. C. Braga, F. Maseras, A. M. Echavarren, *Tetrahedron* **2008**, *64*, 6021.

[21] a) P. H. M. Budzelaar, P. W. N. M. Leeuwen, C. F. Roobeek, *Organometallics* **1992**, *11*, 23; b) F. K. Friedlein, K. Kromm, F. Hampel, J. A. Gladysz, *Chem. Eur. J.* **2006**, *12*, 5267; c) X. Zhao, C. Yeung, V. M. Dong, *J. Am. Chem. Soc.* **2010**, *132*, 5837.

[22] a) P. Fitton, M. P. Johnson, J. E. McKeon, *Chem. Commun.* **1968**, 6; b) P. Fitton, E. A. Rick, *J. Organomet. Chem.* **1971**, *28*, 287; c) B. E. Mann, A. J. Musco, *J. Chem. Soc. Dalton Trans.* **1975**, 1673; d) J. F. Fauvarque, F. Pflüger, M. Troupel, *J. Organomet. Chem.* **1981**, *208*, 419.

[23] a) C. Amatore, E. Carré, A. Jutand, Y. Medjour, *Organometallics* **2002**, *21*, 4540; b) A. Jutand, *Pure Appl. Chem.* **2004**, *76*, 565; c) C. Amatore, E. Carré, A. Jutand, M. A. M′Barki, G. Meyer, *Organometallics* **1995**, *14*, 5605; d) C. Amatore, E. Carré, A. Jutand, *Acta. Chem. Scand.* **1998**, *52*, 100; e) S. Kozuch, S. Shaik, A. Jutand, C. Amatore, *Chem. Eur. J.* **2004**, *10*, 3072; f) C. Amatore, A. Jutand, M. M′Barki, *Organometallics* **1992**, *11*, 3009; g) C. Amatore, E. Carré, A. Jutand, M. A. M′Barki, *Organometallics* **1995**, *14*, 1818.

[24] B. Martín-Matute, C. Mateo, D. J. Cardenas, A. M. Echavarren, *Chem. Eur. J.* **2001**, *7*, 2341.

Received: January 20, 2011
Published online: June 3, 2011

